ELSEVIER

Journal of Computational and Applied Mathematics 94 (1998) 181–197

JOURNAL OF COMPUTATIONAL AND APPLIED MATHEMATICS

# Absolute continuity and spectral concentration for slowly decaying potentials

B.M. Brown *, M.S.P. Eastham, D.K.R. McCormack

*Department of Computer Science, University of Cardiff, Cardiff, CF2 3XF, UK*

Received 25 September 1997; received in revised form 14 April 1998

**Abstract**

We consider the spectral function $\rho(\mu)$ $(\mu \geqslant 0)$ for the Sturm–Liouville equation $y'' + (\lambda - q)y = 0$ on $[0, \infty)$ with the boundary condition $y(0) = 0$ and where $q$ has slow decay $O(x^{-a})$ $(a > 0)$ as $x \to \infty$. We develop our previous methods of locating spectral concentration for $q$ with rapid exponential decay (this Journal 81 (1997) 333–348) to deal with the new theoretical and computational complexities which arise for slow decay. 

*Keywords:* Spectral concentration; Sturm–Liouville problems; Slow-decay potentials

*AMS classification:* 34A12

## 1. Introduction

In a recent paper [5], we gave a new formula

$$\rho'(\mu) = \pi^{-1} s \exp\left(-s^{-1} \int_0^\infty q(x) \sin 2\theta(x, \mu)\, dx\right) \tag{1.1}$$

for the derivative of the spectral function associated with the Sturm–Liouville equation

$$y''(x) + \{\lambda - q(x)\} y(x) = 0 \quad (0 \leqslant x < \infty) \tag{1.2}$$

and the Dirichlet boundary condition

$$y(0) = 0, \tag{1.3}$$

* Correponding author. E-mail: malcolm.brown@cs.cf.ac.uk.

0377-0427/98/$19.00 
*PII* S0377-0427(98)00087-9

the formula applying to the situation where

$$q(x) \in L(0,\infty). \tag{1.4}$$

In (1.1), $\mu > 0, s = \sqrt{\mu}$ and $\theta(x,\mu)$ is the solution of the first-order differential equation

$$\theta'(x,\mu) = s - s^{-1}q(x)\sin^2\theta(x,\mu), \tag{1.5}$$

such that

$$\theta(0,\mu) = 0. \tag{1.6}$$

Also, if (1.3) is replaced by the usual general condition

$$y(0)\cos\alpha + y'(0)\sin\alpha = 0 \quad (0 < \alpha < \pi),$$

the initial factor $s$ in (1.1) is replaced by

$$s\csc^2\alpha(s^2 + \cot^2\alpha)^{-1}$$

and (1.6) is replaced by

$$\theta(0,\mu) = -\tan^{-1}(s\tan\alpha) \quad (-\pi < \theta(0,\mu) < 0).$$

In this paper however, we keep to (1.3) purely for simplicity.

Following [5, 18] (see also [4]), we say that the problem (1.2)–(1.3) exhibits *spectral concentration* at a point $\mu_0$ ($> 0$) if $\rho'$ has a local maximum at $\mu_0$. Then $\rho$ itself has a relatively sharp increase at $\mu_0$. In [5] we used (1.1) to develop computational procedures, based on (1.5) and (1.6), for locating spectral concentration points $\mu_0$ with the emphasis on potentials $q$ which decay rapidly as $x \to \infty$. In particular, we identified a transitional property of $\theta(x,\mu)$ as $\mu$ increases through $\mu_0$ which provides a sensitive test of even slight spectral concentration [5, Sections 2–3]. This property also features in this paper, and we give details of it later at the end of Section 4.

A typical example considered in [5, Section 3.1] and suggested by [20, Example 166] is

$$q(x) = -ce^{-x/4}\cos x \quad (c > 0) \tag{1.7}$$

with exponential decay. However, in [5, Section 5], we pointed out that our procedures are less reliable in cases of slower decay such as

$$q(x) = -c(1+x)^{-a}\cos x \tag{1.8}$$

with $a > 1$, and we also raised the further question of what can be said when $0 < a \leqslant 1$, in which case (1.4) fails and it is no longer clear that (1.1) is available.

In this paper, we deal with these two outstanding matters. First, in Section 2, we show that (1.1) continues to hold in certain situations where (1.4) fails and $q$ is only conditionally integrable on $(0,\infty)$. Certain values of $\mu$ have to be avoided because of the possibility of embedded eigenvalues and discontinuities in $\rho$ but, in $\mu$ – intervals which avoid these values, the spectrum is absolutely continuous. Then, in Section 3, we show how to extend the computational procedures in [5] to locate reliably spectral concentration points for slow-decay examples such as (1.8), with $a \leqslant 1$ allowed.

Finally in this introduction, we note two other approaches to spectral concentration. The software package SLEDGE [9, 19, 20] replaces $q$ in (1.2) by an approximating step-function $\tilde{q}$ over a large

interval $(0,b)$. It then computes the spectral function $\rho(\tilde{q},b,\mu)$ for (1.2) with $\tilde{q}$ and the boundary conditions (1.3) and $y(b)=0$. When refinements of $\tilde{q}$ and $b$ lead to a stable output, the step-function $\rho(\tilde{q},b,\mu)$ provides an approximation to $\rho(\mu)$ to within a prescribed tolerance. SLEDGE is not restricted to (1.4) but, when more explicit formulae such as (1.1) and (1.5) are available, these formulae provide a more sensitive means of detecting spectral concentration [5].

The other approach to spectral concentration lies in the wider theoretical context of quantum resonances and spectral stability [17]. The resonances are nonreal singular spectral points and, in a future paper, we intend to develop the connection between these nonreal points and the real spectral concentration points found in this paper and in [5].

## 2. Absolute continuity of the spectrum

The theory from which (1.1) is derived in [5] was developed in the original work of Titchmarsh [23, Section 5.7] and Weyl [24, p. 264]. This theory uses the fact that, subject to (1.4), there are solutions of (1.1) which together with their derivatives are asymptotic to $\exp(\pm ix\sqrt{\lambda})$ and $\pm i\sqrt{\lambda}\exp(\pm ix\sqrt{\lambda})$ as $x\to\infty$. More recently, the existence of solutions with these or similar asymptotic forms, irrespective of (1.4), provides an application of the subordination theory of Gilbert et al. [13, 21] and leads to the absolute continuity of $\rho(\mu)$ in appropriate intervals. Such asymptotic forms are obtained by transforming (1.2) into a first-order differential system to which the Levinson asymptotic theorem [6, Section 1.3] is applicable, and the necessary transformation methods were developed by Harris, Lutz and Eastham [14–16, 6]. In particular, Behncke [1–3] used the transformations in [15] to establish the absolute continuity for potentials such as (1.8) when $a>\frac{1}{3}$ provided that certain resonance values of $\mu$ are avoided. In this section, we use the transformation due to Eastham and McLeod [6, Sections 4.6–4.7], [12] to both extend this result and establish (1.1) for all $a>0$.

In [6, (4.1.8)] (1.2) is considered with $\lambda=1$ and, therefore, some minor changes are required in the transformation theory as presented in [6, Section 4.6]. As in [6, Section 4.1], we take $q$ to have the form

$$q(x)=\xi(x)p(x), \tag{2.1}$$

where $p$ has period $2\pi$ and

$$\xi(x)\to 0 \ \ (x\to\infty), \ \ \xi'(x)\in L(0,\infty).$$

Also,

$$\xi(x)\notin L^M(0,\infty), \ \ \xi(x)\in L^{M+1}(0,\infty) \tag{2.2}$$

for some integer $M$ $(\geqslant 1)$. Thus $\xi(x)=(1+x)^{-a}$ $(0<a\leqslant 1)$ is the simplest example. The appropriate formulation of (1.2) as a system is

$$W'(x)=\{i\Lambda_0+R(x)\}W(x) \tag{2.3}$$

where, as in [6, Section 4.1],

$$\Lambda_0=\mathrm{dg}(\sqrt{\lambda},-\sqrt{\lambda}), \ \ R(x)=-i\xi(x)p(x)D\Omega \tag{2.4}$$

with $D = \mathrm{dg}(\frac{1}{2}, -\frac{1}{2})$ and $\Omega$ having all entries unity. The connection between $y$ and $W$ is

$$\begin{pmatrix} y \\ y' \end{pmatrix} = \begin{pmatrix} 1 & 1 \\ \mathrm{i}\sqrt{\lambda} & -\mathrm{i}\sqrt{\lambda} \end{pmatrix} W. \tag{2.5}$$

The resonance set $\sigma$ in [6, (4.1.18)] is now replaced by

$$\sigma = \{N^2/4; N = 1, 2, ...\}. \tag{2.6}$$

We can now proceed as in [6, Lemma 4.6.1] with a transformation

$$W = \{\exp(\xi P_1 + \xi^2 P_2 + ... + \xi^M P_M)\} Z, \tag{2.7}$$

where the matrices $P_m$ have period $2\pi$, $\mathrm{dg} P_m = 0$, and $M$ is as in (2.2). This takes (2.3) into

$$Z' = (\mathrm{i}\Lambda_0 + \xi\Lambda_1 + ... + \xi^M \Lambda_M + S)Z, \tag{2.8}$$

where $S \in L(0, \infty)$ and $\Lambda_m$ is diagonal with period $2\pi$. Here $\lambda$ is excluded from the set $\sigma$ in (2.6). Further, since $R$ has trace zero in (2.4), it follows that

$$\mathrm{tr}\, \Lambda_m = -\mathrm{tr}\, P'_m = 0 \quad (m \geqslant 1)$$

as in [6, Lemma 4.9.2 (i)]. Thus $\Lambda_m$ has the form

$$\Lambda_m = \mathrm{dg}(\lambda^{(m)}, -\lambda^{(m)}).$$

Finally, when $\lambda$ is real and positive, the conditions of [6, Theorem 4.6.1] are satisfied by (2.3) and (2.4), and then the $\Lambda_m$ are all pure imaginary.

The method used in [23, Section 5.7] for obtaining the Titchmarsh–Weyl $m(\lambda)$ function and the spectral function $\rho(\mu)$ can be adapted to the situation which we have now in (2.1)–(2.8). We note that (2.7) has the form

$$W = (I + Q)Z, \tag{2.9}$$

where $Q(x) = o(1)$ $(x \to \infty)$, and we choose $X$ so that $(I + Q)^{-1}$ exists in $[X, \infty)$. We also note that (2.8) is

$$Z' = (\Lambda + S)Z, \tag{2.10}$$

where $\Lambda$ has the form

$$\Lambda = \mathrm{dg}(v, -v) \tag{2.11}$$

with

$$v = \mathrm{i}\sqrt{\lambda} + \mathrm{o}(1) \quad (x \to \infty). \tag{2.12}$$

Further, $v$ is pure imaginary when $\lambda$ is real and positive.

The usual integral form of (2.10) is

$$Z(x) = \Phi(x)Z(X) + \int_X^x \Phi(x)\Phi^{-1}(t)S(t)Z(t)\,\mathrm{d}t$$

with

$$\Phi(x) = \exp\left\{\mathrm{dg}\left(\int_X^x v(t)\,\mathrm{d}t, -\int_X^x v(t)\,\mathrm{d}t\right)\right\}. \tag{2.13}$$

Then, by (2.9), the solutions of (2.3) satisfy

$$W(x) = \{I + Q(x)\}\Phi(x)\{I + Q(X)\}^{-1}W(X) + \{I + Q(x)\}\int_X^x \Phi(x)\Phi^{-1}(t)\tilde{S}(t)W(t)\,\mathrm{d}t, \tag{2.14}$$

where

$$\tilde{S} = S(I + Q)^{-1} \in L(X, \infty). \tag{2.15}$$

If $\lambda$ and $\sqrt{\lambda}$ satisfy $0 \leqslant \arg\lambda < \pi$ and $0 \leqslant \arg\sqrt{\lambda} < \frac{1}{2}\pi$, it follows immediately from (2.12)–(2.15) and a Gronwall inequality that $W(x)\exp\left(\int_X^x v(t)\,\mathrm{d}t\right)$ is bounded on $[X, \infty)$. To use this property in the integral term in (2.14), we define $I_1 = \mathrm{dg}(1, 0)$ and $I_2 = \mathrm{dg}(0, 1)$ in order to split the two entries in $\Phi$ in (2.13). Then, by (2.14), we have

$$W(x) = \{I_2 B(\lambda) + \mathrm{o}(1)\}\exp\left(-\int_X^x v(t)\,\mathrm{d}t\right) \quad (x \to \infty)$$

when $\lambda$ is nonreal, where

$$B(\lambda) = \{I + Q(X)\}^{-1}W(X) + \int_X^\infty \exp\left(\int_X^t v(u)\,\mathrm{d}u\right)\tilde{S}(t)W(t)\,\mathrm{d}t$$

(cf. [23, (5.7.5)–(5.7.8)]). Also, when $\lambda$ has a real and positive value $\mu$, (2.14) again gives

$$W(x) = I_1 A(\mu)\exp\left(\int_X^x v(t)\,\mathrm{d}t\right) + I_2 B(\mu)\exp\left(-\int_X^x v(t)\,\mathrm{d}t\right) + \mathrm{o}(1),$$

where $v$ is now pure imaginary and $A(\mu)$ is the same as $B(\mu)$ but with $-v$ instead of $v$ (cf. [23, (5.7.2)–(5.7.3)]). Finally, in terms of the first component $a(\mu)$ of $A(\mu)$ and the second component $b(\lambda)$ of $B(\lambda)$, the transformation (2.5) back to $y$ gives

$$y(x) = \{b(\lambda) + \mathrm{o}(1)\}\exp\left(-\int_X^x v(t)\,\mathrm{d}t\right) \tag{2.16}$$

for $\lambda$ nonreal and, when $\lambda = \mu$,

$$\begin{aligned} y(x) &= a(\mu)\exp\left(\int_X^x v(t)\,\mathrm{d}t\right) + b(\mu)\exp\left(-\int_X^x v(t)\,\mathrm{d}t\right) + \mathrm{o}(1), \\ y'(x) &= \mathrm{i}\sqrt{\mu}a(\mu)\exp\left(\int_X^x v(t)\,\mathrm{d}t\right) - \mathrm{i}\sqrt{\mu}b(\mu)\exp\left(-\int_X^x v(t)\,\mathrm{d}t\right) + \mathrm{o}(1). \end{aligned} \tag{2.17}$$

We now have the same type of asymptotic formulae as in [23, Section 5.7], from which (1.1) follows as in [5]. We indicate the details briefly, the only proviso being that $\mu \notin \sigma$ in (2.6) as already mentioned.

Let $y_1(x,\lambda)$ and $y_2(x,\lambda)$ be the solutions of (1.2) which satisfy the initial conditions

$$y_1(0,\lambda)=1,\quad y_1'(0,\lambda)=0,\quad y_2(0,\lambda)=0,\quad y_2'(0,\lambda)=1,$$

and let $a_1,b_1,a_2,b_2$ denote the corresponding multipliers as in (2.16) and (2.17). Then $y_1+my_2\in L^2(0,\infty)$ gives

$$m(\lambda)=-b_1(\lambda)/b_2(\lambda)\quad(\mathrm{im}\lambda\neq 0) \tag{2.18}$$

as in [23, (5.7.9)]. When $\lambda=\mu$, $y_1$ and $y_2$ are real-valued and, hence,

$$a_j(\mu)=\overline{b_j(\mu)}\ (j=1,2)$$

in (2.17). Then $W(y_1,y_2)=1$ gives

$$\mathrm{im}(\overline{b_2}b_1)(\mu)=-(4\sqrt{\mu})^{-1}.$$

Hence, by (2.18),

$$\begin{aligned}\lim_{\lambda\to\mu}\mathrm{im}\ m(\lambda)&=\{4\sqrt{\mu}\mid b_2(\mu)\mid^2\}^{-1}\\&=\lim_{x\to\infty}\{\mu^{1/2}y_2^2(x,\mu)+\mu^{-1/2}y_2'^2(x,\mu)\}^{-1}\end{aligned}$$

by (2.17) and (1.1) follows as in [5].

Finally in this section, we note that the requirement $\mu\notin\sigma$ can be relaxed as follows when $M=1$ in (2.2). Let $c_n$ $(-\infty<n<\infty)$ denote the complex Fourier coefficients of $p(x)$ in (2.1). Then it is shown in [6, Section 4.2] ( see also [7]) that (2.17) continuous to hold when $\mu=\frac{1}{4}N^2$ for some $N$ provided that $c_N=0$. Thus, altogether, (1.1) is valid

1. for all $\mu>0$ when $\xi\in L(0,\infty)$,
2. for all $\mu>0$ except those $\mu=\frac{1}{4}N^2$ for which $c_N\neq 0$, when $M=1$ in (2.2),
3. for $\mu>0$ and $\mu\notin\sigma$ when $M\geqslant 2$ in (2.2).

## 3. An integration algorithm

We aim to compute $\rho'$ in (1.1) to within a reasonable degree of accuracy such as $10^{-5}$. The error in $\rho'$ is of course made up of a number of components: the truncation error due to the approximation of the semi-infinite interval by a finite interval, the error inherent in the solving algorithm of the differential equation and the rounding error due to the rational approximation of real numbers in computer arithmetic. We focus here on the truncation error and rely on the standard theory for both the error in the Runge–Kutta algorithm as well as the floating-point numerical software on our computer system. The infinite integral in (1.1) is of course truncated at a suitable value $X_0$. However, to achieve a truncation error of $10^{-6}$ in the integrand when, for example, $a=3$ in (1.8) requires $X_0=10^3$, and integration over the large range $(0,10^3)$ is unreliable. The situation is much worse for smaller values of $a$. In this section, we develop an iterative algorithm which accelerates the convergence of the integral in (1.1) and enables us to cope with potentials such as (1.8) when $a>0$.

Guided by the example (1.8), we give the algorithm for the case $p(x) = \cos x$, so that (2.1) is

$$q(x) = \xi(x)\cos x \tag{3.1}$$

and $\xi(x)$ is as before but with $M \geqslant 0$ in (2.2). Our methods also cover the more general situation where $p(x)$ is a finite Fourier series, but the details become more complicated. We require the following trigonometric identity, valid for any $\alpha, \beta, \theta$ and $x$:

$$\begin{aligned} &8\cos x \sin^2\theta \sin(\alpha\theta + \beta x) \\ &\quad = 2\sin\{\alpha\theta + (\beta+1)x\} + 2\sin\{\alpha\theta + (\beta-1)x\} \\ &\qquad - \sin\{(\alpha+2)\theta + (\beta+1)x\} - \sin\{(\alpha-2)\theta + (\beta-1)x\} \\ &\qquad - \sin\{(\alpha+2)\theta + (\beta-1)x\} - \sin\{(\alpha-2)\theta + (\beta+1)x\}. \end{aligned} \tag{3.2}$$

This is easily verified, and there is a similar identity with $\cos(\alpha\theta + \beta x)$ on the left and all cosines on the right.

Next, we require the following integrals over $[0, \infty)$ with $\theta$ as in (1.1), $F \in L(0, \infty)$ and $F(\infty) = 0$:

$$\begin{aligned} I(F, \alpha, \beta) &= \int F(x)\sin(\alpha\theta + \beta x)\,dx \\ J(F, \alpha, \beta) &= \int F(x)\cos(\alpha\theta + \beta x)\,dx \\ K(F, \alpha, \beta) &= \int F(x)\cos x \sin^2\theta \sin(\alpha\theta + \beta x)\,dx \\ L(F, \alpha, \beta) &= \int F(x)\cos x \sin^2\theta \cos(\alpha\theta + \beta x)\,dx. \end{aligned} \tag{3.3}$$

It follows from (1.5), (3.1) and an integration by parts that

$$\begin{aligned} &(\alpha s + \beta) I(F, \alpha, \beta) \\ &\quad = \int F \sin(\alpha\theta + \beta x)(\alpha\theta' + \beta + \alpha s^{-1}\xi \cos x \sin^2\theta)\,dx \\ &\quad = F(0) + J(F', \alpha, \beta) + \alpha s^{-1} K(F\xi, \alpha, \beta) \end{aligned} \tag{3.4}$$

and, similarly,

$$(\alpha s + \beta) J(F, \alpha, \beta) = -I(F', \alpha, \beta) + \alpha s^{-1} L(F\xi, \alpha, \beta). \tag{3.5}$$

Finally in these introductory formulae, it follows from (3.2) and (3.4) that

$$\begin{aligned} 8K(F, \alpha, \beta) = {} & 2I(F, \alpha, \beta+1) + 2I(F, \alpha, \beta-1) \\ & - I(F, \alpha+2, \beta+1) - I(F, \alpha-2, \beta-1) \\ & - I(F, \alpha+2, \beta-1) - I(F, \alpha-2, \beta+1) \end{aligned} \tag{3.6}$$

$$\begin{aligned} 8L(F,\alpha,\beta) = {} & 2J(F,\alpha,\beta+1)+2J(F,\alpha,\beta-1) \\ & -J(F,\alpha+2,\beta+1)-J(F,\alpha-2,\beta-1) \\ & -J(F,\alpha+2,\beta-1)-J(F,\alpha-2,\beta+1). \end{aligned} \tag{3.7}$$

We can now return to the integral in (1.1), which we denote by $I_0$. Then, by (3.1), we can write

$$2I_0 = I(\xi,2,1)+I(\xi,2,-1). \tag{3.8}$$

By (3.4) and (3.6), the two $I-$integrals here can be expressed in terms of $I$ and $J$ integrals with integrands containing $\xi'$ and $\xi^2$. These last integrals converge more rapidly than those in (3.8) for cases such as

$$\xi(x) = (\text{const.})(1+x)^{-a}. \tag{3.9}$$

Repetition of the algorithm (3.4)–(3.7) accelerates the convergence by introducing integrands with higher derivatives and higher powers of $\xi$.

Certain values of $\mu$ have to be excluded to avoid a zero factor $\alpha s+\beta$ on the left-hand side of (3.4) and (3.5). Thus, with $\alpha = 2$ and $\beta = -1$ in (3.8), we exclude

$$\mu = \tfrac{1}{4} \tag{3.10}$$

at the first implementation of the algorithm. At the next application of the formulae (3.4) and (3.5) the value

$$\mu = 1 \tag{3.11}$$

is also excluded and, at the third application of (3.4) and (3.5), the additional values

$$\tfrac{1}{36},\quad \tfrac{1}{16},\quad \tfrac{9}{16},\quad \tfrac{9}{4}. \tag{3.12}$$

We note that there is an overlap of these values and the $N^2/4$ values discussed at the end of Section 2 for the validity of (1.1) when $M \geqslant 1$.

## 4. Implementing the algorithm

In this section we show how the integration algorithm from Section 3 is used to identify points of spectral concentration for potentials of the form

$$q(x) = -c(1+x)^{-a}\cos x \tag{4.1}$$

given by (3.1) and (3.9), where $c > 0$ and $a > 0$. The algorithm is implemented using both symbolic methods and numerical approximations.

We recall from (3.8) that the integral which appears in the formula for $\rho'$ is the sum of two integrals $I(\xi,2,1)$ and $I(\xi,2,-1)$. The first part of the algorithm consists of a procedure to improve the convergence of these integrals. We focus first on the case $a \geqslant 2$ and then comment on the procedure that we have been forced to adopt for smaller values of $a$.

First an acceptable order of convergence $\varepsilon$ is decided upon: we have chosen $\varepsilon = x^{-6}$. A purpose written Mathematica code is used to repeatedly apply the integration by parts formulae (3.4)–(3.7) to

the integrals whose integrands are larger then $\varepsilon$. Starting with the integrals $I(\xi,2,1)$ and $I(\xi,2,-1)$, the integration by parts formulae generate integrals of the types $I,J,K,L$ (cf. (3.4)) whose integrands have smaller order than the integrand in (1.1) together with terms that do not involve the variable $x$. This procedure is repeated until all integrands have order less than or equal to $\varepsilon$. Thus Mathematica is used to generate a symbolic formula which consists of terms that do not depend upon $x$, denoted by $C(\mu)$, together with a sum of integrals of type (3.4). Next a Mathematica code is written to parse the formula and reconstruct the integrands. The symbolic formula is finally converted into a Fortran 77 function which for convenience we denote by $F(x,\mu)$.

The next task is to evaluate the integral (1.1) numerically from the improved integrand for each value of $\mu$ under consideration. As the integral $I_0$ depends upon $\theta$, which itself is a solution of the differential equation (1.5), this is done by solving the system

$$\begin{pmatrix} I_0(x,\mu) \\ \theta(x,\mu) \end{pmatrix}' = \begin{pmatrix} F(x,\mu) \\ s - s^{-1}q(x)\sin^2\theta \end{pmatrix} \tag{4.2}$$

over $[0,X]$ for some large $X$, where $I_0(x,\mu)$ is the integral over $(0,x)$ in (1.1), subject to the initial conditions

$$I_0(0,\mu) = C(\mu), \quad \theta(0,\mu) = 0,$$

typically $X=100$ has been used in our example.

There are several practical difficulties encountered in performing the above tasks. First, the improvements in the convergence of the integrals brought about by the integration by parts generate a large number of integrals $I,J,K,L$ as indicated by the right-hand sides of (3.6) and (3.7). Numerical inaccuracies do not allow us at the moment to improve the integrands beyond a certain point. The inaccuracies arise from the $K$- and $L$-type integrals when we attempt to improve the integrand beyond $\xi^3$. The combined integrand $F(x,\mu)$ therefore involves

$$\xi'''', \ \xi\xi''', \ \xi\xi'', \ \xi^2\xi', \ \xi'^2, \ \xi^3 \tag{4.3}$$

and the excluded values of $\mu$ are $\frac{1}{4}$ and 1 as stated in (3.10) and (3.11). We have also tried to perform the numerical integration by extending the system of differential equations (4.2) to one in which each entry is only one of the integrands of $I,J,K,L$ together with the defining equation for $\theta$. However this procedure, which has required a more sophisticated parsing routine to be written, has produced no significant improvement in the results.

When $a \geqslant 2$, the order of convergence $\varepsilon = x^{-6}$ is achieved by the $F(x,\mu)$ indicated by (4.3). When $a < 2$, we continue to use the same $F(x,\mu)$ but with a consequent increase in the truncation error. However, the increased error leads to two complications which become more serious as $a$ decreases. The first complication is that (1.1) only gives the approximate location of the spectral concentration points. The second and more serious complication is that spurious maxima of $\rho'$ are produced, the more so as $a$ decreases, and therefore it is necessary to identify the true maxima. We resolve these difficulties by using a transitional property of $\theta(x,\mu)$ which we now describe.

As reported in [4, Section 2] ( see also [5]), spectral concentration at a point $\mu_0$ is indicated by a certain transitional behaviour of $\theta(x,\mu)$ as $\mu$ increases through $\mu_0$. Let $(x_1,x_2)$ be an interval in which the Sturm–Liouville coefficient $\mu - q(x) < 0$ and $\mu'$ and $\mu''$ be suitably close to a point of $\mu_0$

of spectral concentration with $\mu' < \mu_0 < \mu''$. Then we expect the integral in (1.1) to be large and negative — and therefore producing spectral concentration — if

$$(N + \tfrac{1}{2})\pi < \theta(x, \mu_0) < (N + 1)\pi \tag{4.4}$$

in $(x_1, x_2)$, where $N(\geqslant 0)$ is an integer. We find that, particularly in situations of sharp concentration, (4.4) is realised with the following features:

1. $\theta(x, \mu')$ and $\theta(x, \mu'')$ are close together for $0 \leqslant x \leqslant x_1$ with their values at $x_1$ close to $(N + \frac{1}{2})\pi$.
2. $\theta(x, \mu'') - \theta(x, \mu')$ is close to $\pi$ for $x$ to the right of $x_2$, with $\theta(x, \mu'')$ close to $(N + \frac{3}{2})\pi$.
3. $\theta(x, \mu_0)$ is close to $(N + 1)\pi$.

Thus the graph of $\theta(x, \mu)$ undergoes a rapid transition in $(x_1, x_2)$ as $\mu$ increases from $\mu'$ to $\mu''$. The transitional behaviour is illustrated by the graphs in the next section.

We return now to $F(x, \mu)$ in (4.3) and the case $a < 2$. The first complication, concerning the approximate location of spectral concentration points, is resolved by using this approximate location as the starting point of a search range for $\mu$ within which (1.5) is solved numerically for $\theta(x, \mu)$. Then the points $\mu_0$ at which the transition occurs can be located more precisely. We can also use the transition property of $\theta(x, \mu)$ even when $a \geqslant 2$ to verify independently that true spectral concentration points obtained precisely as the local maxima of $\rho'$ are not artifacts of our methods. At the same time, any apparent maxima which are not associated with the transition property are rejected as spurious. We find that, as $a$ decreases, the number of spurious maxima increases significantly making the task of rejection a major (but unseen) part of our work.

Finally in these comments, we note that there is a further complication as a result of the excluded values $\mu = \frac{1}{4}, 1, \frac{1}{36}, \ldots$ in (3.10)–(3.12). Although it is clear from the integration by parts formulae (3.4)–(3.7) that our methods of evaluating $\rho'$ must exclude these points, the numerical realisation of our algorithm produces unreliable results in neighbourhoods of these points. Again we test these neighbourhoods for the appearance of the transitional behaviour of $\theta(x, \mu)$. We refer also to [4, Section 6] for a similar use of $\theta(x, \mu)$ in a different but related situation where a direct formula for $\rho'$ poses difficulties.

In the case of (4.1), the intervals $(x_1, x_2)$ in (4.4) are approximately

$$((2r + \tfrac{1}{2})\pi, (2r + \tfrac{3}{2})\pi) \quad (r = 0, 1, 2, \ldots). \tag{4.5}$$

We then denote $\mu_0$ in (4.4) by

$$\mu(c, N)\ (r = 0),\ \nu(c, N)\ (r = 1),\ \xi(c, N)\ (r = 2)$$

and, in the next section, we record our findings concerning the location of these points when $c(> 0)$ is regarded as a parameter. We shall also comment on higher values of $r$ as appropriate.

## 5. Examples

### 5.1. Example: $a = 2$ in (4.1)

Here $q(x)$ is $L(0, \infty)$ and (1.1) is valid for all $\mu > 0$. We apply the algorithm as described in (4.3) and we have to exclude values of $\mu$ near to $\frac{1}{4}$ and 1 in the computation of $\rho'(\mu)$. In Table 1

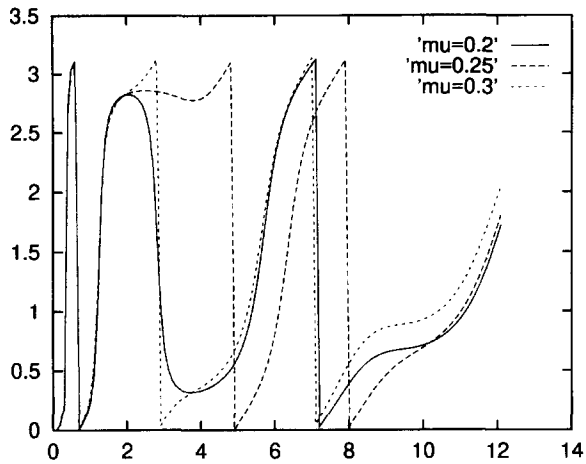


Fig. 1. $\theta$ graph for $\mu(49.26,1) = 0.25$.

Table 1
$a = 2$

| $c$ | $\mu(c,0)$ | $\mu(c,1)$ | $\mu(c,2)$ | $\mu(c,3)$ | $\nu(c,3)$ |
|---|---|---|---|---|---|
| 2 | 0.45 | | | | |
| 7 | 0.26 | 2.05 | | | |
| 9 | 0.08 | 2.41 | | | |
| 20 | | 2.10 | | | |
| 30 | | 1.87 | 5.28 | | |
| 40 | | 1.29 | 5.51 | | |
| 50 | | 0.15 | 5.10 | | 0.68 |
| 60 | | | 4.81 | | 0.72 |
| 70 | | | 4.73 | 9.75 | 0.70 |
| 80 | | | 4.45 | 9.95 | 0.67 |
| 100 | | | 3.11 | 9.26 | 0.60 |
| 120 | | | 0.80 | 8.9 | 0.52 |
| 125 | | | 0.10 | 8.84 | 0.49 |

we list the spectral concentration points which we have located as giving local maxima of $\rho'(\mu)$ except that, as mentioned in Section 4, we have located points near to $\frac{1}{4}$ and 1 by identifying the value of $\mu$ which is associated with the transitional property of $\theta(x,\mu)$. Thus, for example, Fig. 1 gives the graphs of $\theta(x,\mu)$ which identify $\mu(49.26,1) = 0.25$ and provide part of the evolution of $\mu(c,1)$ as $c$ varies which is summarised in the second column of Table 1. We point out that the graphs represent $\theta \pmod{\pi}$, whence the repeated cut-offs at the ordinate $\pi$.

When $c$ has the particular value 122.1, we find that

$$\mu(c,2) = \nu(c,3) = 0.51.$$

Thus, the two local maxima of $\rho'$ arising from $\mu(c,2)$ and $\nu(c,3)$ coalesce or, equivalently, two different intervals $(x_1,x_2)$ ( with $r = 0$ and $r = 1$) simultaneously make relatively large contributions

to the integration in (1.1). One result of this coalescence is that $\nu(c,3)$ becomes $\nu(c,4)$ when $c > 122.1$. Thus, the last-line entry 0.49 in Table 1 is in fact $\nu(125,4)$.

### 5.2. Example: $a = 1$ in (4.1)

Now, $M = 1$ at the end of Section 2, and (1.1) is valid for all $\mu > 0$ except $\mu = \frac{1}{4}$. We have followed the procedure for $a < 2$ as described in Section 4, in which the excluded values are $\mu = \frac{1}{4}$ (again) and $\mu = 1$. We find that spectral concentration points occur in greater profusion than for $a = 2$, and our results for $c \leqslant 100$ are given in Tables 2 and 3. Coalescing points occur as follows:

$$\begin{aligned} &\mu(c,1) = \nu(c,3) = 1.98, \quad (c = 24.25),\\ &\mu(c,1) = \xi(c,4) = 0.53, \quad (c = 31.2),\\ &\mu(c,2) = \nu(c,5) = 4.02, \quad (c = 64.6) \end{aligned} \tag{5.1}$$

as well as

$$\mu(c,3) = \nu(c,8) = 10.06, \quad (c = 106).$$

As $c$ increases through these respective values, the oscillation number $N$ for $\nu(c,N)$ or $\xi(c,N)$ increases by one, because of the transition $\pi$ in the values of $\theta$ caused by the $\mu$ spectral concentration points. This increase is indicated at the tops of columns in Table 3. Also, in Fig. 2, we give the $\theta$-graphs which show the transitional behaviour twice to illustrate the coalescence of $\mu(c,2)$ and $\nu(c,5)$ when $c = 64.6$.

Table 2
$a = 1$

| $c$ | $\mu(c,0)$ | $\mu(c,1)$ | $\mu(c,2)$ | $\mu(c,3)$ | $\mu(c,4)$ |
|---|---|---|---|---|---|
| 2 | 0.5 | | | | |
| 3 | 0.48 | 3.05 | | | |
| 4 | 0.41 | 2.73 | | | |
| 5 | 0.26 | 2.68 | | | |
| 6 | 0.03 | 2.68 | | | |
| 10 | | 2.76 | 6.77 | | |
| 15 | | 2.97 | 6.81 | | |
| 20 | | 2.61 | 6.84 | | |
| 25 | | 1.85 | 7.09 | 12.51 | |
| 30 | | 0.80 | 7.36 | 12.73 | |
| 40 | | | 7.35 | 12.82 | 18.38 |
| 50 | | | 6.43 | 13.36 | 20.41 |
| 60 | | | 4.89 | 13.90 | 20.55 |
| 70 | | | 2.89 | 13.92 | 20.79 |
| 80 | | | 1.75 | 13.36 | 21.39 |
| 90 | | | 1.55 | 12.35 | 22.06 |
| 100 | | | 1.31 | 11.01 | 22.47 |

Table 3
$a = 1$

| $c$ | $\nu(c,2)$ | $\nu(c,3/4)$ | $\nu(c,5/6)$ | $\nu(c,8)$ | $\xi(c,4/5)$ |
|---|---|---|---|---|---|
| 2 | | | | | |
| 3 | | | | | |
| 4 | | | | | |
| 5 | 0.70 | | | | |
| 6 | 0.75 | | | | |
| 10 | 0.72 | | | | |
| 15 | 0.59 | | | | |
| 20 | 0.41 | 2.22 | | | 0.69 |
| 25 | 0.14 | 2.06 | | | 0.64 |
| 30 | | 2.05 | 4.05 | | 0.57 |
| 40 | | 1.83 | 4.10 | | 0.34 |
| 50 | | 1.46 | 4.15 | | 0.19 |
| 60 | | 1.00 | 4.08 | | 0.04 |
| 70 | | 0.43 | 3.88 | | |
| 80 | | | 3.60 | | |
| 90 | | | 3.24 | | |
| 100 | | | 2.82 | 10.14 | |

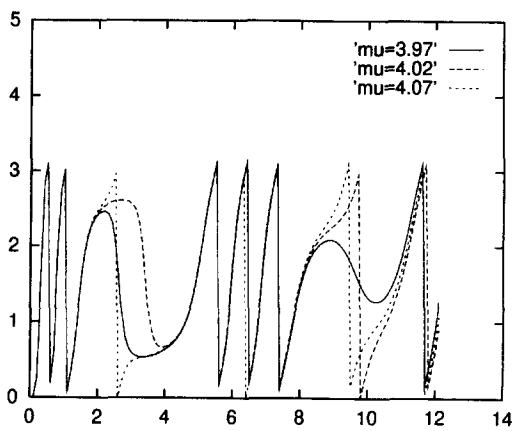


Fig. 2. $\theta$ graphs for $\mu(64.6,2) = \nu(64.6,5) = 4.02$.

### 5.3. Example: $a = \frac{1}{2}$ in (4.1)

We have intimated in Sections 2 and 4 that slow decay spawns theoretical and computational complexities, the latter including the task of segregating the large number of spurious and actual local maxima of $\rho'$. This task is expensive in computer time and, therefore, we have restricted the range of $c$ in this part of our investigation to $0 < c \leqslant 30$. Our findings for $\mu, \nu$ and $\xi$ points are summarised in Table 4, in which figures are given to more than two decimal places when necessary to distinguish between closely situated points.

Table 4
$a = \frac{1}{2}$

| $c$ | $\mu(c,0)$ | $\mu(c,1)$ | $\mu(c,2)$ | $\nu(c,1)$ | $\nu(c,2)$ | $\nu(c,3\backslash 4)$ | $\xi(c,2)$ | $\xi(c,3)$ | $\xi(c,4)$ | $\xi(c,5)$ |
|---|---|---|---|---|---|---|---|---|---|---|
| 2 | 0.61 | | | 0.56 | | | | | | |
| 3 | 0.50 | | | 0.487 | 0.73 | | 0.4869 | 0.62 | | |
| 4 | 0.26 | | | | 0.72 | | | 0.66 | 0.78 | |
| 6 | | | | | 0.575 | 1.83 | | 0.569 | 0.71 | |
| 8 | | 3.49 | | | 0.33 | 2.08 | | 0.331 | 0.58 | 1.85 |
| 10 | | 3.61 | | | 0.09 | 2.11 | | | | 2.01 |
| 15 | | 3.11 | | | | 1.842 | | | | 1.841 |
| 20 | | 2.0 | 8.82 | | | 1.2986 | | | | 1.2984 |
| 25 | | 0.51 | 9.02 | | | 0.59 | | | | |
| 30 | | | 8.72 | | | | | | | |

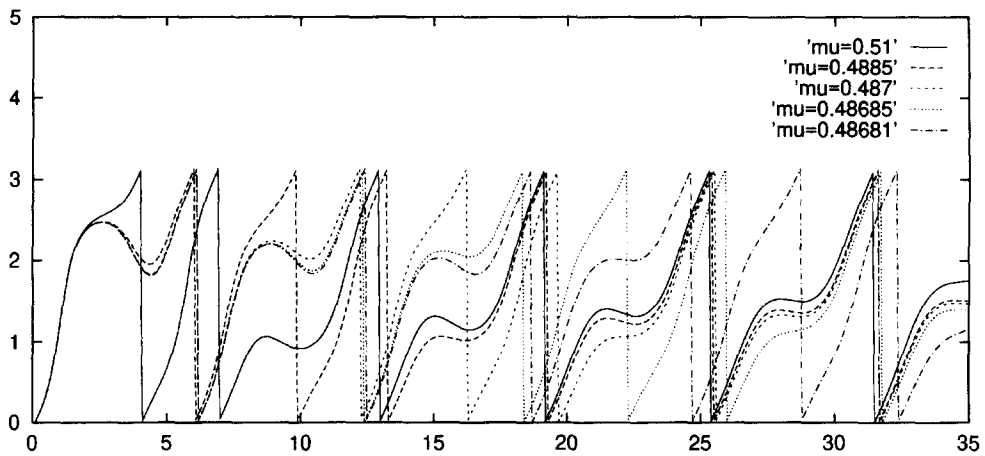


Fig. 3. $\theta$ graphs for $a = \frac{1}{2}, c = 3$.

In particular, we find that there are two values of $c$ and $\mu$ in whose neighbourhoods several very close (but apparently not coalescing) points of spectral concentration exsist. The values are

$$c = 3, \quad \mu = 0.49; \quad c = 5.5, \quad \mu = 0.66.$$

In the case of $c = 3$, for example, we have evidence for the existence of at least seven such spectral concentration points, corresponding to $0 \leqslant r \leqslant 6$ in (4.5). In Fig. 3, we exhibit this evidence for $0 \leqslant r \leqslant 4$. The figure shows $\theta$–graphs for a decreasing sequence of values of $\mu$ (all close to 0.49) where the transition occurs for $r = 0, 1, 2, 3, 4$ in turn. We make a further comment on this matter in Section 6.3 below.

For $c$ in the stated range $(0, 30)$ we have identified one pair of coalescing points which, as in Section 5.2, are associated with a change in the oscillation number $N$, as follows: $\mu(c,1) = \nu(c,3) = 0.67$ $(c = 24.5)$. Further, in addition to what is reported in Table 4, we have found that, for $15 \leqslant c \leqslant 24.5$, there is a $\nu(c,4)$ which is almost identical to $\mu(c,1)$. Thus, for $c$ in this range, we have a spectral concentration point which enjoys contributions from both $r = 0$ and $r = 1$ in

(4.5). This linkage between $\mu$ and $v$ points is a new feature for $a = \frac{1}{2}$ and it poses the question whether there is a theoretical explanation.

## 6. Concluding remarks

### 6.1. Absence of spectral concentration

In [5, Section 5], we made the following conjecture concerning the appearance of spectral concentration for (1.2) and (1.3) when $q(x)$ has the form $cQ(x)$ $(c > 0)$ such as we have in (1.7), (1.8) and (4.1).

**Conjecture 6.1.** *Let $Q(x) < 0$ in some interval $(0, x_0)$. Let $Q(x)$ change sign one or more times as $x$ increases with $Q(x)$ finally decaying to zero as $x \to \infty$ and $Q(x) \in L(0, \infty)$. Then there is a number $c_0$ $(> 0)$ such that spectral concentration does not appear for any $\mu > 0$ when $c$ lies in the range $(0, c_0)$.*

For the example (1.7) we showed in [5] that the conjecture is true with $0.28 < c_0 \leqslant 0.29$ and, more generally, an affirmative answer to the conjecture has been given recently for the special case of (2.1) in which $x\xi(x)$ is $L(0, \infty)$. Thus (4.1) is covered provided that $a > 2$. The conjecture remains undecided when $1 < a \leqslant 2$ in (4.1), although our computational findings for $a = 2$ indicate that $c_0$ exists with $1.0 < c_0 \leqslant 1.1$.

### 6.2. More general potentials

There is no difficulty, in principle, in extending our methods for (2.1) to potentials which are a finite sum

$$q(x) = \sum_{1}^{L} \xi_l(x) p_l(x) \tag{6.1}$$

and the $p_l(x)$ have different periods $\omega_l$, provided that the $\omega_l$ are mutually commensurable. The $p_l(x)$ would then all have a common basic period $\omega$, and the set $\sigma$ in (2.6) is modified to

$$\sigma = \{N^2\pi^2/\omega^2; N = 1, 2, \ldots\}. \tag{6.2}$$

However, in the absence of a special form such as (2.1) or (6.1), it is no longer clear what can be said, in general, about the absolutely continuous nature of $\rho$ when $q$ fails to be $L(0, \infty)$. There is no simple exceptional set $\sigma$ such as (6.2) because in [10, Section 4.4], [11, 22] it is shown that, given any set of isolated positive real numbers $\mu_n$ and given $a$ $(0 < a < 1)$, there is a potential $q(x) = O(x^{-a})$ $(x \to \infty)$, such that the spectral function has discontinuities at the $\mu_n$.

### 6.3. Higher values of r in (4.5)

We have focused on $r = 0, 1, 2$ in (4.5) in order to establish our computational methods and, consequently, we have located mainly $\mu, v$ and $\xi$ points of spectral concentration. Thus, we have

largely confined our search for the transitional behaviour of $\theta(x,\mu)$ to the $x-$range $(0,18)$. There remains the question, on which we have touched in the remarks relating to Fig. 3, whether $\theta(x,\mu)$ possesses the transitional property also for higher values of $r$ and, more particularly, whether an infinity of values of $r$ is involved in this way for some fixed value of $c$. Thus we have the theoretical question of whether an infinite set (bounded or unbounded) of spectral concentration points can exist for some $c$. All that is known is that an unbounded set cannot occur when $a > 2$ because it is shown in [8] that the set of spectral concentration points is bounded for any $q$ in (1.2) such that $xq(x)$ is $L(0,\infty)$.

## References

[1] H. Behncke, Absolute continuity of Hamiltonians with von Neuman Wigner potentials, Proc. Amer. Math. Soc. 111 (1991) 373–384.
[2] H. Behncke, Absolute continuity of Hamiltonians with von Neuman Wigner potentials II, Manuscripta Math. 71 (1991) 163–181.
[3] H. Behncke, The $m$-function for Hamiltonians with Wigner von Neumann potentials, J. Math. Phys. 35 (4) (1994) 1445–1462.
[4] B.M. Brown, M.S.P. Eastham, D.K.R. McCormack, Spectral concentration and perturbed discrete spectra, J. Comp. Appl. Math. 86 (1997) 415–425.
[5] B.M. Brown, M.S.P. Eastham, D.K.R. McCormack, Spectral concentration and rapidly decaying potentials, J. Comp. Appl. Math. 81 (1997) 333–348.
[6] M.S.P. Eastham, The asymptotic solution of linear differential systems, London Math. Soc. Monographs 4, Clarendon Press, Oxford, 1989.
[7] M.S.P. Eastham, The number of resonant states in perturbed harmonic oscillation, Quart. J. Math. Oxford (2), 42 (1991) 49–55.
[8] M.S.P. Eastham, On the location of spectral concentration for Sturm–Liouville problems with rapidly decaying potentials, Mathematika 45 (1998) 25–36.
[9] M.S.P. Eastham, C.T. Fulton, S.A. Pruess, Using the SLEDGE package on Sturm-Liouville problems having nonempty essential spectrum, ACM Trans. Math. 22 (1996) 423–446.
[10] M.S.P. Eastham, H. Kalf, Schrödinger-type operators with continuous spectra, Research Notes in Mathematics vol. 65, Pitman, London, 1982.
[11] M.S.P. Eastham, J.B. McLeod, The exsistence of eigenvalues embedded in the continuous spectrum of ordinary differential operators, Proc. Roy. Soc. Edinb. 79A (1977) 25–34.
[12] M.S.P. Eastham, J.B. McLeod, Non-resonance for linear differential systems, Proc. Roy. Soc. Edinb. 111A (1989) 103–122.
[13] D.J. Gilbert, D.B. Pearson, On subordinary and analysis of the spectrum of one-dimensional Schrödinger operators, J. Math. Anal. Appl. 128 (1987) 30–56.
[14] W.A. Harris, D.A. Lutz, On the asymptotic integration of linear differential systems, J. Math. Anal. Appl. 48 (1974) 1–16.
[15] W.A. Harris, D.A. Lutz, Asymptotic integration of adiabatic oscillators, J. Math. Anal. Appl. 51 (1975) 76–93.
[16] W.A. Harris, D.A. Lutz, A unified theory of asymptotic integration, J. Math. Anal. Appl. 57 (1977) 571–586.
[17] P.D. Hislop, I.M. Sigal, Introduction to spectral theory, Springer Applied Math. Sciences vol. 113, 1996.
[18] M. Marletta, The detection of quantum-mechanical resonances using the Pruess method, Technical Note ACM 90-14, Royal Military College of Science, 1990.
[19] S.A. Pruess, C.T. Fulton, Mathematical software for Sturm–Liouville problems, ACM Trans. Math. Software, 19 (1993) 360–376.
[20] S.A. Pruess, Y. Xie, C.T. Fulton, Performance of the Sturm–Liouville software package SLEDGE, Colorado School of Mines Department of Math. and Comp. Sci. Tech. Rep. MCS-91-19, 1991.
[21] G. Stolz, Bounded solutions and absolute continuity of Sturm–Liouville operators, J. Math. Anal. Appl. 169 (1992) 210–228.

[22] C.R. Thurlow, M.S.P. Eastham, The exsistence of eigenvalues of infinite multiplicity for the Schrödinger operator, Proc. Roy. Soc. Edinb. 86A (1980) 61–64.
[23] E.C. Titchmarsh, Eigenfunction expansions, Part I, 2nd ed., Clarendon Press, Oxford, 1962.
[24] H. Weyl, Über gewöhnliche Differentialgleichungen mit Singularitäten und die zugehörigen Entwicklungen willkürlicher Funktionen, Math. Annln. 68 (1910) 220–269.